

Amino Substituted Bisketenes: Generation, Structure, and Reactivity

Nanyan Fu, Annette D. Allen, Shinjiro Kobayashi, Thomas T. Tidwell,* and Sinisa Vukovic

Department of Chemistry, University of Toronto, Toronto, Ontario M5S 3H6, Canada

Selvananthan Arumugam and Vladimir V. Popik

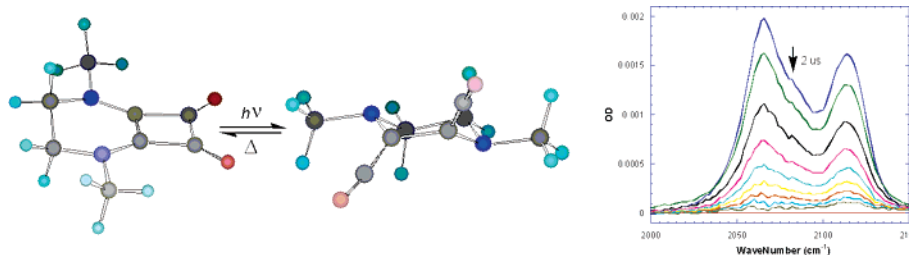
Department of Chemistry, University of Georgia, Athens, Georgia 30602-2556

Masaaki Mishima

Institute for Materials Chemistry and Engineering, 6-10-1 Hakozaki, Fukuoka, 812-8581 Japan

ttidwell@chem.utoronto.ca

Received October 9, 2006



Hitherto unknown diamino-substituted bisketenes with both free (**14**) and tethered (**16**) amino substituents have been generated by using laser flash photolysis for ring opening of the corresponding cyclobutenediones. The time-resolved kinetics of ring closure of the amino bisketenes back to the cyclobutenediones were measured by IR or UV spectroscopy, and give first-order rate constants which vary by a factor of 7.5×10^4 , and the bis(Me₂N) bisketene **14** is the most reactive in ring closure that has been reported. Rate constants for ring closure of these and previously observed bisketenes vary by a factor of 10^{13} . The dialkylamino bisketenes **16** (R = Me, *n*-Bu) with tethered substituents and restricted geometries are less reactive than the bis(Me₂N) bisketene **14** by factors of 1700 and 540, respectively. Computational results obtained with DFT methods suggest angle strain in the tethered cyclobutenediones **15** inhibits facile cyclization of bisketenes **16**.

Introduction

The first report of both the direct observation and the isolation of amino-substituted ketenes has recently appeared,^{1a} although these species have been sought since the early days of ketene chemistry.^{1b} The acyclic ketenes **1** and the cyclic derivative **2** were prepared by the room temperature reaction of the corresponding stable carbenes with carbon monoxide, and the structures were confirmed by spectroscopic evidence, and for the crystalline products **1b** and **2** by X-ray crystallography (Scheme 1).¹ Reactivity studies of these species have not been reported, but their isolation at room temperature is highly unusual for ketenes with amino, oxygen, or halo substituents.

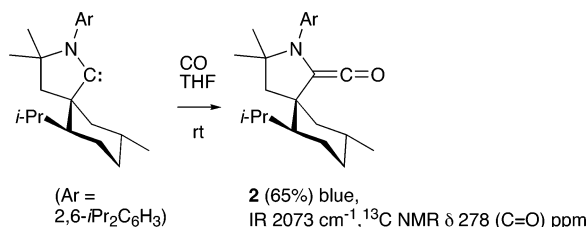
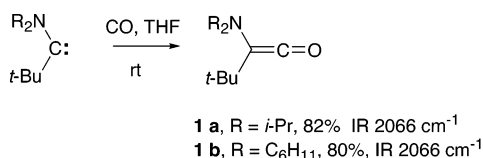
Aminoketenes have been calculated to be destabilized,² and the stability of the amino-substituted ketenes **1** and **2** is attributable to steric protection by the bulky substituents. Computations indicate that the parent aminoketene (**3**) is most stable with pyramidalized nitrogen so that the lone pair is in the ketene plane as is found in **1b**, and the *syn*- and *anti*-periplanar geometries **3a,b** are close in energy.^{1,2} The coplanar structure **3c** with the lone pair parallel to the ketene π system is calculated to be less stable and not an energy minimum,^{1,2} but the rigid planar ring forces this geometry for **2**.¹

The favored nitrogen pyramidalization and coplanar alignment of the orbital containing the nitrogen lone electron pair in

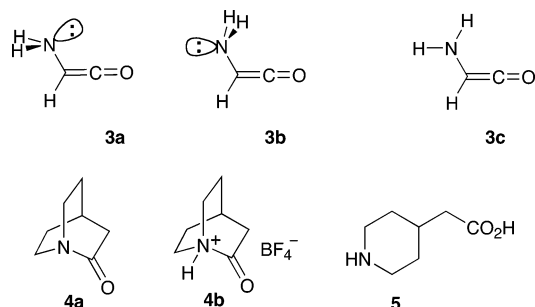
(1) (a) Lavallo, V.; Canac, Y.; Donnadiou, B.; Schoeller, W. W.; Bertrand, G. *Angew. Chem., Int. Ed.* **2006**, *45*, 3488–3491. (b) For a commentary see: Tidwell, T. T. *Angew. Chem., Int. Ed.* **2006**, *45*, 5580–5582.

(2) (a) Gong, L.; McAllister, M. A.; Tidwell, T. T. *J. Am. Chem. Soc.* **1991**, *113*, 6021–6028. (b) McAllister, M. A.; Tidwell, T. T. *J. Org. Chem.* **1994**, *59*, 4506–4515. (c) Gupta, V. P.; Sharma, A.; Agrawal, S. G. *Bull. Korean Chem. Soc.* **2006**, *27*, 1297–1304. (d) Badawi, H. M. *J. Mol. Struct.* **2005**, *726*, 253–260.

SCHEME 1. Generation of Stable Aminoketenes



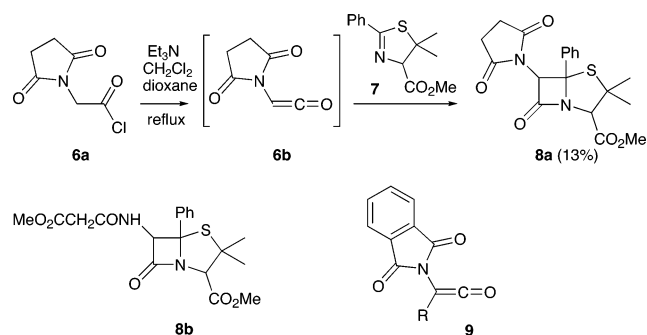
aminoketenes contrasts with the favored parallel arrangement of the electron pair containing the p orbital of nitrogen to the adjacent carbonyl group π bond in amides.³ The strong preference for the conjugated geometry in amides is highlighted by the recent first preparation of a well-characterized tetrafluoroborate salt **4b** of the parent 2-quinuclidone structure **4a**.^{3a} The parent amide **4a** lacking normal amide conjugation has so far not been observed from **4b**, which reacts with $t_{1/2} < 15$ s with water forming ring opened **5** or a salt as the only observed product.^{3a} Smaller deviations from planarity of the amide nitrogen in 7-azabicyclo[2.2.1]heptane amides have been attributed to CNC angle strain and allylic strain.^{3d}



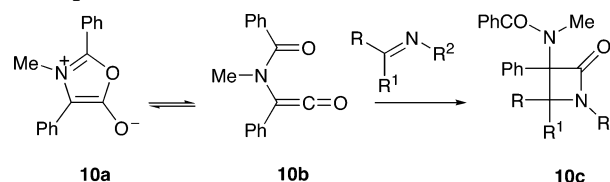
After early speculation about nitrogen-substituted ketenes⁴ these ultimately proved to be of significant utility in the race to prepare penicillins, and evidently the first reported successful preparation of a nitrogen-substituted ketene was reported by Sheehan and co-workers.⁵ The reaction of succinimidoacetyl chloride **6a** with triethylamine generated ketene **6b** as an unobserved intermediate that was captured in situ by ketene–imine [2+2] cycloaddition with the thiazoline **7** forming **8a** (Scheme 2), which was used in the synthesis of the 5-phenyl penicillin **8b**.^{5,6} Phthalimidoketene **9** (R = H) was generated and trapped in a similar fashion.⁶

Amido-substituted ketenes were considered as possible intermediates in these reactions,^{6a,b} and it is now generally

SCHEME 2. Amidoketene Generation



SCHEME 3. Münchnone–Amidoketene Interconversion and Capture



accepted that highly reactive ketenes are usually formed under these conditions, but are often too short-lived for direct observation.^{4d,6d,e} Many further examples of nitrogen-substituted ketenes, including aminoketenes, have been generated by analogous procedures, especially for use in β -lactam formation.^{6b–d} Winter and Pracejus prepared substituted phthalimidoketenes **9** by dehydrochlorination of the corresponding acyl chlorides with *tertiary* amines, and evidence for ketene formation for R = Bn, Ph, and *i*-Pr in solution was provided by the observation of characteristic ketene bands at 2141, 2136, and 2125 cm^{-1} , respectively,^{7a} while the ketene with R = *t*-Bu was obtained as a solid: mp 96–98 °C, IR 2134 cm^{-1} .^{7a} Steric protection from the two bulky groups and delocalization of the amido nitrogen lone pair evidently permit this to be stable even in the solid state.

Münchnone **10a** was proposed to exist in equilibrium with a low concentration of the amidoketene **10b**, which was not observed directly but underwent [2+2] cycloaddition with imines forming β -lactams **10c** (Scheme 3).^{7b} Further examples of such Münchnone–amidoketene equilibria have recently been reported.^{7c,d}

Cyclobutenediones **11** have been extensively utilized for the generation of 1,2-bisketenes **12**. When the bisketenes possess ketene-stabilizing silyl substituents they are of comparable or greater stability compared to **11**, and the transformations may be carried out thermally.^{4d,8c,d} With less electropositive substituents the bisketenes **12** are less stable than the cyclobutenediones **11**, but may be generated by photolysis, and their conversion

(3) (a) Tani, K.; Stoltz, B. M. *Nature* **2006**, *441*, 731–734. (b) For a commentary see: Wasserman, H. H. *Nature* **2006**, *441*, 699–700. Also see ref 3c. (c) Clayden, J.; Moran, W. J. *Angew. Chem., Int. Ed.* **2006**, *45*, 7118–7120. (d) Otani, Y.; Nagae, O.; Naruse, Y.; Inagaki, S.; Ohno, M.; Yamaguchi, K.; Yamamoto, G.; Uchiyama, M.; Ohwada, T. *J. Am. Chem. Soc.* **2003**, *125*, 15191–15199.

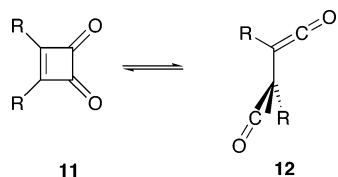
(4) (a) Staudinger, H.; Kupfer, O. *Ber. Dtsch. Chem. Ges.* **1911**, *44*, 1638–1640. (b) Staudinger, H.; Anthes, E.; Schneider, H. *Ber. Dtsch. Chem. Ges.* **1913**, *46*, 3539–3531. (c) For a review of recent developments in ketene chemistry see: Tidwell, T. T. *Eur. J. Org. Chem.* **2006**, 563–576. (d) Tidwell, T. T. *Ketenes*, 2nd ed.; Wiley: Hoboken, NJ, 2006.

(5) (a) Sheehan, J. C.; Buhle, E. L.; Corey, E. J.; Laubach, G. D.; Ryan, J. J. *J. Am. Chem. Soc.* **1950**, *72*, 3828–3829. (b) Sheehan, J. C.; Laubach, G. D. *J. Am. Chem. Soc.* **1951**, *73*, 4376–4780.

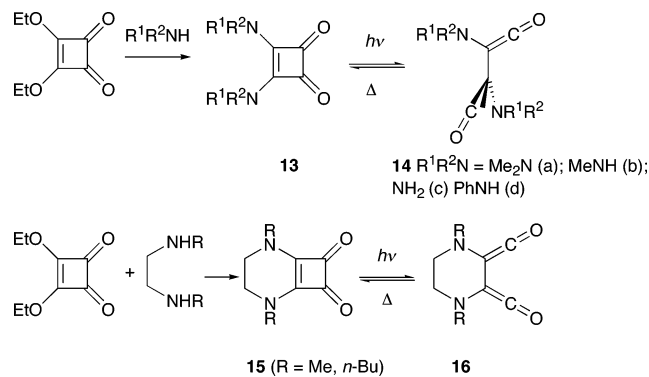
(6) (a) Sheehan, J. C.; Ryan, J. J. *J. Am. Chem. Soc.* **1951**, *73*, 1204–1206. (b) Sheehan, J. C.; Ryan, J. J. *J. Am. Chem. Soc.* **1951**, *73*, 4367–4372. (c) Sheehan, J. C.; Corey, E. J. *Org. React.* **1957**, *9*, 388–408. (d) Palomo, C.; Aizpurua, J. M. *Science of Synthesis (Houben-Weyl)*; Bellus, D., Danheiser, R., Eds.; Thieme Verlag: Stuttgart, Germany, 2006; Vol. 23.6. (e) Reichen, W. *Chem. Rev.* **1978**, *78*, 569–588.

(7) (a) Winter, S.; Pracejus, H. *Chem. Ber.* **1966**, *99*, 151–159. (b) Huisgen, R.; Funke, E.; Schaefer, F. C.; Knorr, R. *Angew. Chem., Int. Ed.* **1967**, *6*, 367–368. (c) Dhawan, R.; Dghaym, R. D.; Arndtsen, B. A. *J. Am. Chem. Soc.* **2003**, *125*, 1474–1475. (d) Dhawan, R.; Dghaym, R. D.; St. Cyr, D. J.; Arndtsen, B. A. *Org. Lett.* **2006**, *8*, 3927–3930.

SCHEME 4. Cyclobutenedione–Bisketene Interconversion



SCHEME 5. Preparation of Amino-Substituted Cyclobutenediones 13 and 15, and Conversion to Bisketenes 14 and 16



back to **11** may be observed spectroscopically, including derivatives with ketene destabilizing chlorine and oxygen substituents (Scheme 4).^{4d,8} Aminocyclobutenediones have been extensively studied,⁹ and are biologically active,^{9g} with applications in materials chemistry,^{9c} but have not previously been examined as bisketene precursors.

Results

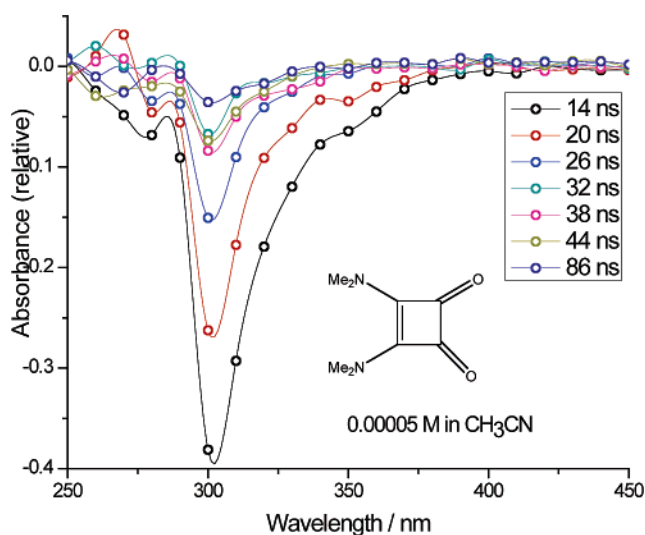
Diamino-substituted cyclobutenediones⁹ with both free (**13a**, $R^1R^2N = Me_2N$; **13b**, $R^1R^2N = MeNH$; **13c**, $R^1R^2N = NH_2$; **13d**, $R^1R^2N = PhNH$) and tethered (**15**, R = Me, *n*-Bu) substituents were prepared from substitution reactions of amines or 1,2-diamines, respectively, with diethoxycyclobutenedione (Scheme 5). The X-ray structure of the tethered cyclobutenedione **15** (R = Me) was determined, as shown in Figure S5 (Supporting Information), and conversions to the bisketenes **14** and **16** were carried out by using laser flash photolysis (Scheme 4).

Upon laser flash photolysis of **13** and **15** in CH_3CN and other solvents with previous techniques^{8c,10a,b} the respective bisketenes **14** and **16** were generated as transient species, and the kinetics of reformation of the cyclobutenediones were measured by the increase in the UV absorption at wavelengths given with the observed rate constants in Table 1. A representative kinetic trace, for the reformation of the UV absorbance for **13a** in CH_3CN , is shown in Figure 1. The variation of the rate constants with solvent polarity $CH_3CN > CCl_4 > isoctane$ is similar to that

TABLE 1. Rate Constants for Ring Closure of Bisketenes **14** and **16** at 25 °C

substituents	method, solvent	k (s^{-1})
Me_2N (14a)	UV, ^a CH_3CN	$(9.58 \pm 0.38) \times 10^7$
MeNH (14b)	UV, ^b CH_3CN	$(1.84 \pm 0.32) \times 10^5$
NH_2 (14c)	UV, ^c CH_3CN	$(1.28 \pm 0.13) \times 10^3$
PhNH (14d)	UV, ^a CH_3CN	$(6.72 \pm 0.25) \times 10^6$
16 (R = Me)	UV, ^d CH_3CN	$(5.54 \pm 0.27) \times 10^4$
	UV, ^e $CDCl_3$	$(1.58 \pm 0.08) \times 10^4$
	UV, ^e isoctane	$(5.86 \pm 0.34) \times 10^3$
16 (R = <i>n</i> -Bu)	UV, ^f CH_3CN	$(1.64 \pm 0.06) \times 10^5$
	IR, ^g CH_3CN	$(1.82 \pm 0.08) \times 10^5$
		1.77×10^5 (average) ^h
	UV, ^e $CDCl_3$	$(4.02 \pm 0.20) \times 10^4$
	UV, ^e isoctane	$(1.04 \pm 0.02) \times 10^4$

^a Monitoring wavelength 330 nm. ^b Monitoring wavelength 289 nm. ^c Monitoring wavelength 280 nm. ^d Monitoring wavelength 300 and 283 nm. ^e Monitoring wavelength 315 and 275 nm. ^f Monitoring wavelength 290 nm. ^g Monitoring wavelength 2064, 2116 cm^{-1} . ^h Average of the IR and UV rate constants.

FIGURE 1. Recovery of UV absorption of cyclobutenedione **13** ($R^1R^2N = Me_2N$) from the bisketene **14** formed by laser flash photolysis.

observed for other bisketenes, which was attributed to greater polarity of the incipient product cyclobutenediones.^{8d}

The identification of the bisketene **16** (R = *n*-Bu) was confirmed by observation of distinctive ketenyl IR bands at 2064 and 2116 cm^{-1} in CH_3CN (Figure 2), and the kinetics of the decay of this absorption were measured by IR, and gave a rate constant in good agreement with the value measured by UV for reformation of the cyclobutenedione **15** (Table 1).

Selected reactions were also examined computationally with use of DFT methods at the B3LYP/6-31G(d) level, using

(8) (a) Allen, A. D.; McAllister, M. A.; Tidwell, T. T.; Zhao, D. *Acc. Chem. Res.* **1995**, *115*, 265–271. (b) Allen, A. D.; Lough, A. J.; Tidwell, T. T. *Chem. Commun.* **1996**, 2171–2172. (c) Allen, A. D.; Colomvakos, J. D.; Egle, I.; Luszyk, J.; McAllister, M. A.; Tidwell, T. T.; Wagner, B. D.; Zhao, D.-c. *J. Am. Chem. Soc.* **1995**, *117*, 7552–7553. (d) Allen, A. D.; Colomvakos, J. D.; Diederich, F.; Egle, I.; Luszyk, J.; McAllister, M. A.; Rubin, Y.; Tidwell, T. T.; Wagner, B. D.; Zhao, D.-c. *J. Am. Chem. Soc.* **1997**, *119*, 12045–12050. (e) Aguilar-Aguilar, A.; Allen, A. D.; Peña-Cabrera, E.; Fedorov, A.; Fu, N.; Henry-Riyad, H.; Kobayashi, S.; Leuninger, J.; Schmid, U.; Tidwell, T. T.; Verma, R. *J. Org. Chem.* **2005**, *71*, 9556–9561. (f) McAllister, M. A.; Tidwell, T. T. *J. Am. Chem. Soc.* **1994**, *116*, 7233–7238.

(9) (a) Frontera, A.; Morey, J.; Oliver, A.; Piña, M. N.; Quiñero, D.; Costa, A.; Ballaster, P.; Deya, P. M.; Anslyn, E. V. *J. Org. Chem.* **2006**, *71*, 7185–7195. (b) Muthyala, R. S.; Subramanian, G.; Todaro, L. *Org. Lett.* **2004**, *6*, 4663–4665. (c) Lunelli, B.; Rovarsi, P.; Ortoleva, E.; Destro, R. *J. Chem. Soc., Faraday Trans.* **1996**, *92*, 3611–3623. (d) Griffiths, G. R.; Rowe, M. D.; Webb, G. A. *J. Mol. Struct.* **1971**, *8*, 363–371. (e) Maahs, G.; Hegenberg, P. *Angew. Chem., Int. Ed.* **1966**, *5*, 888–893. (f) Thorpe, J. E. *J. Chem. Soc. B* **1968**, 435–436. (g) Verniest, G.; Colpaert, J.; Törnøos, K. W.; De, Kimpe, N. *J. Org. Chem.* **2005**, *70*, 4549–4552. (h) Ehrhardt, H.; Hünig, S.; Pütter, H. *Chem. Ber.* **1977**, *110*, 2506–2523.

(10) (a) Allen, A. D.; Fedorov, A. V.; Najafian, K.; Tidwell, T. T.; Vukovic, S. *J. Am. Chem. Soc.* **2004**, *126*, 15777–15783. (b) Acton, A. W.; Allen, A. D.; Antunes, L. M.; Fedorov, A. V.; Najafian, K.; Tidwell, T. T.; Wagner, B. D. *J. Am. Chem. Soc.* **2002**, *124*, 13790–13794. (c) *Gaussian 98*, Revision A-9; Gaussian, Inc.: Pittsburgh, PA, 1998.

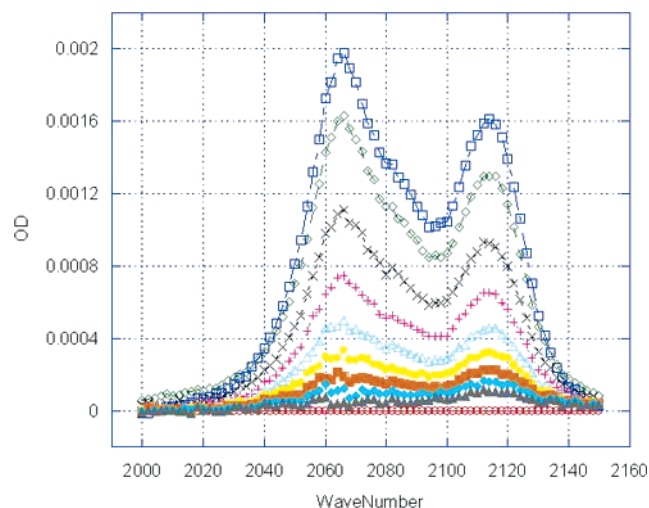
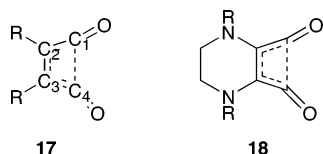


FIGURE 2. Decay of IR absorption (2- μ s intervals between curves) of bisketene **16** ($R = n$ -Bu) forming cyclobutenedione **15**.

Gaussian 98.^{10c} These methods have proven to be reliable in other recent studies of ketene reactions.^{10a,b} For comparison, cyclobutenediones **11**, $R = H$ and Me, were also studied. The energies of cyclobutenediones **13** and **15**, the corresponding bisketenes **14** and **16**, and the transition states **17** and **18** for



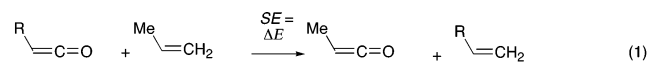
their interconversion were obtained, and the energy changes are summarized in Table 2. Details of the energies and geometries are given in Tables S3–S5 (Supporting Information). The results for **11** and **12** ($R = H$) are in reasonable agreement with previously obtained ab initio results at the MP2/6-31G* level: $E_{\text{rel}}(\text{TS}) = 30.8$ kcal/mol, $E_{\text{rel}}(\mathbf{12}) = 3.2$ kcal/mol, $\Delta E^*(\text{ring closure}) = 27.6$ kcal/mol.^{8f}

Discussion

The measured rate constants for ring closure of the bisketenes **14** are large in all cases, with relative rate constants of 7.5×10^4 , 5.2×10^3 , 140, and 1.0 for $R^1R^2N = \text{Me}_2\text{N}$, PhNH, MeNH, and NH_2 , respectively. The rate constant for ring closure for **14a** ($R^1R^2N = \text{Me}_2\text{N}$) is the greatest that has been measured for any 1,2-bisketene, of 30 examples, and even exceeds by a factor of 5000 that for **20** forming **19** (Scheme 6), in which there is a gain in aromatic stabilization for forming the substituted benzene ring. The rate constant for **14a** ($R^1R^2N = \text{Me}_2\text{N}$) is greater than that of **12** (substituents Me_3Si and Me), the least reactive bisketene for which we have measured a rate constant, by a factor of 2×10^{13} , and exceeds that estimated for **12** ($R = \text{Me}_3\text{Si}$) by a factor of 10^{18} .^{8d} These results demonstrate the powerful ketene destabilizing effect and cyclobutenedione stabilization by amino groups.

The effect of substituents on ketene stability has been previously examined by using computed isodesmic energy parameters (SE) (in kcal/mol) for substituents on ketenes, calculated from eq 1.^{8d} These gave a fair correlation of rate constants for ring closure of 19 bisketenes in isoctane or $\text{CH}_3\text{-CN}$. However, it was also considered that the reactivities might

be affected by a separate resonance effect of the substituents on the ketenyl moieties and the incipient product cyclobutenediones in the transition states. Particularly for π -electron donor substituents such as OH and NH_2 , these might be expected to enhance bisketene ring closure due to their strong π -electron donor character. This latter effect would be related to σ_p^+ parameters. Therefore for the larger set of 25 substrates with substituent parameters now available both one and two parameter correlations were tested, as shown in eqs 2 and 3,



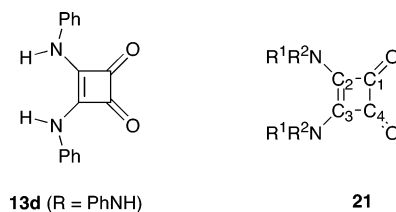
$$\log k(\text{bisketene}) = -(0.31 \pm 0.02)\Sigma SE - (1.63 \pm 0.31) \quad r = 0.94 \quad (2)$$

$$\log k(\text{bisketene}) = -(0.29 \pm 0.03)\Sigma SE - (0.41 \pm 0.38)\Sigma \sigma_p^+ - (1.94 \pm 0.42) \quad r = 0.94 \quad (3)$$

respectively. However, it may be seen that the correlation coefficients are essentially the same, and furthermore that the error in the dependence upon the σ_p^+ parameters is quite large. Thus specific inclusion of the latter effect does not improve the correlation, and the reactivity is best correlated by the SE parameters alone (Figure 3). While this was unexpected it appears that the effect of the π -electron donating ability of the substituents is already included in the SE parameters. The relevant SE and σ_p^+ parameters used are compiled in Table S6 (Supporting Information).

The reactivities of the amino-substituted cyclobutenediones **14** ($R^1R^2N = \text{Me}_2\text{N}$, PhNH, MeNH, and NH_2) are not well accounted for by this correlation, as the reactivities differ by a factor of 7.5×10^4 , but computations (Table S7, Supporting Information) indicate these substituents have very similar SE values. Calculated barriers for ring closure (Table 2) do, however, predict the relative reactivities in ring closure for **14** ($R^1R^2N = \text{Me}_2\text{N}$, MeNH, and NH_2), as discussed below.

The structure of the cyclobutenedione **13** ($R^1R^2N = \text{PhNH}$) has been proposed to have a *syn* arrangement of the phenyls relative to carbonyl groups.^{9b} This structure would be favored for steric reasons, and our computation indicates **13** ($R^1R^2N = \text{MeNH}$) has a similar structure in the most stable conformation, although a planar structure with the Me group *anti* to the carbonyl oxygen is also a minimum energy structure. Our computed structure for **13** ($R^1R^2N = \text{Me}_2\text{N}$) (Figure S5, Supporting Information) indicates an essentially coplanar structure, with dihedral angles of 174.2° for $\text{C}_1\text{C}_2\text{C}_3\text{N}$ and -8.4° for $\text{NC}_2\text{C}_3\text{N}$ (numbering as in **21**). No evidence has been found in reported structures of bis(diamino) cyclobutenediones **13** or **15** obtained by computation or X-ray of intramolecular hydrogen bonding interactions involving the amino groups.



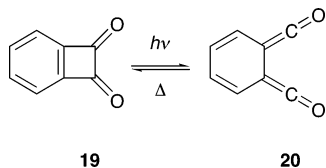
The variation in the relative rates for ring closure of **14** ($R^1R^2N = \text{Me}_2\text{N}$, PhNH, MeNH, and NH_2) of $7.5 \times 10^4:5.2 \times 10^3:140:1$ is striking. The electron donor effect of the groups in stabilizing the incipient cyclobutenediones as measured by

TABLE 2. B3LYP/6-31G(d) Calculated Relative Energies (kcal/mol)^a for Interconversion of Cyclobutenediones **11**, **13**, or **15** with Bisketenes **12**, **14** or **16**, Respectively, and Rate Constants for Ring Closure

cyclobutenedione	$E_{\text{rel}}(\mathbf{11}, \mathbf{13}, \text{ or } \mathbf{15})$	$E_{\text{rel}}(\text{TS})$	$E_{\text{rel}}(\mathbf{12}, \mathbf{14}, \text{ or } \mathbf{16})$	$\Delta E^*(\text{ring closure})$	$k \text{ (s}^{-1}\text{) } 25^\circ\text{C}$ CH ₃ CN
11 (R = H)	0.00	28.42	1.74	26.68	<i>b</i>
11 (R = Me)	0.00	33.32	14.55	18.77	3.60×10^{-2} ^c
13 (R ¹ R ² N = Me ₂ N)	0.00	38.84	35.54	3.30	9.58×10^7
13 (R ¹ R ² N = MeNH)	0.00	42.83	36.85	5.98	1.84×10^5
13 (R ¹ R ² N = NH ₂)	0.00	42.54	35.25	7.29	1.28×10^3
15 (R = H)	0.00	45.92	32.67	13.25	<i>b</i>
15 (R = Me)	0.00	50.31	37.99	12.32	5.54×10^4

^a With ZPVE. ^b Not determined. ^c Reference 8d.

SCHEME 6. Interconversion of Benzocyclobutenone **19** and Bisketene **20**



the respective σ_p^+ constants¹¹ of -1.70 , -1.40 , -1.81 , and -1.30 , respectively, would contribute to this difference, although the data for R = MeNH do not fit the trend. However, the σ_p^+ constant for this substituent^{11c} was obtained in a separate study by a different laboratory than the others, and this may cause the inconsistency. The calculated barriers for ring closure of **14** (R¹R²N = Me₂N, MeNH, and NH₂) of 3.30, 5.98, and 7.29 kcal/mol, respectively, fit very well with the experimental results.

The X-ray structure of the tethered cyclobutenedione **15** (R = Me) (Figure S5, Supporting Information) clearly shows the near planar geometry at the amino substituents with sp² hybridization at nitrogen to permit conjugative electron donation to the cyclobutenedione ring. In the calculated structure of the derived bisketene the nitrogen has, however, assumed a pyramidalized geometry (sum of the C–N–C bond angles 338.7°), which reduces the destabilizing conjugative interaction of the amino substituents and the ketyl groups. Sums of calculated bond angles at nitrogen for bisketenes **14** are 341.5° (R¹R²N = Me₂N), 336.6° (R¹R²N = MeNH), and 330.4° (R¹R²N = NH₂), showing increasing planarization of the nitrogen with increasing substitution. This trend is consistent with a steric effect as the nitrogen becomes more heavily substituted.¹²

The tethered diamino-substituted bisketenes **16** (R = Me and *n*-Bu) have similar rate constants for ring closure, and these are the same as or smaller than those of the free bisketenes **14** (R¹R²N = Me₂N, PhNH, and MeNH), but larger than that for **14** (R¹R²N = NH₂). As the tethered bisketenes **16** may appear constrained to conformations closer to the coplanar geometries of the cyclobutenediones, it might have been expected that these would have enhanced reactivity in ring closure compared to acyclic analogues. The calculated barrier (Table 2) for ring

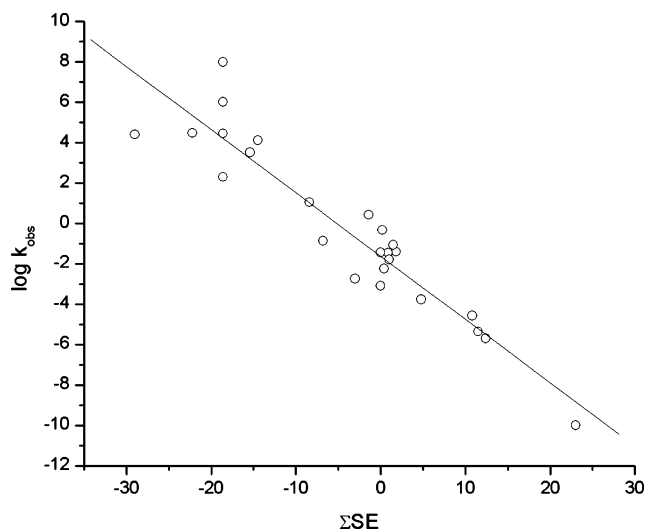


FIGURE 3. Correlation of rate constants for bisketene ring closure with ketene stabilization parameters SE.

closure of the tethered bisketene **16** (R = Me) of 12.32 kcal/mol is greater than those of **14** (R¹R²N = Me₂N, MeNH, and NH₂), and as noted above the experimental results follow the calculated barriers, except for **14** (R¹R²N = NH₂).

Examination of the calculated bond distances of the reactants, transition states, and products as defined in Table S4 and structure **21** reveals that the cyclobutenediones **11** with R = H or Me have cyclobutene-like structures, with C₂C₃ bond lengths of 1.355 and 1.368 Å, while C₁C₂ and C₁C₄ range from 1.508 to 1.587 Å. However, for amino-substituted cyclobutenediones **13** (R¹R²N = Me₂N, MeNH, or NH₂) and for the tethered analogues **15** (R = H, CH₃) there is a trend toward equalization of the bond distances, with longer C₂C₃ bonds and shorter C₁C₂ and C₃C₄ bonds, consistent with conjugative electron donation from nitrogen to the ring. In the transition states for ring closure the length of the forming C₁C₄ bond is greater for the amino-substituted derivatives than for **11** (R = H, CH₃), consistent with the lower barriers and earlier transition states for ring closure of the amino bisketenes. The dihedral bond angles C₁C₂C₃C₄ between the forming ketyl groups in the transition states are 21.6° and 26.9° for the cyclobutenedione precursors **11** (R = H and Me, respectively) and 29.7° (Me₂N), 29.8° (MeNH), and 29.8° (NH₂) for the corresponding amino-substituted derivatives, also consistent with the earlier transition states and lower barriers for ring closure of the latter group. For the tethered derivative from **15** (R = Me), this angle is 26.0°, suggesting a greater barrier for ring closure than for the other amines, consistent with experiment. For the bisketenes the C₁C₂C₃C₄ dihedral angles (Table S4) range from 78.3° to 74.4° for **12** (R = H,

(11) (a) Brown, H. C.; Okamoto, Y. *J. Am. Chem. Soc.* **1958**, *80*, 4979–4987. (b) Hansch, C.; Leo, A.; Taft, R. W. *Chem. Rev.* **1991**, *91*, 165–195. (c) Epstein, L. M.; Ashkinadze, L. D.; Shubina, E. S.; Kravtsov, D. N.; Kazitsyna, L. A. *J. Organomet. Chem.* **1982**, *228*, 53–59.

(12) In ref 3d the sum of the bond angles at nitrogen in amides, designated as θ , and the hinge angle α (the angle between the bond to the carbonyl group in amides and the plane defined by the nitrogen atom and the two other substituents) are designated as measures of the planarity of the nitrogen atom. The angle α has values of 138.18, 130.25, and 128.08 for **14** (R¹R²N = Me₂N, MeNH, and NH₂, respectively), consistent with the trend in the sum of the bond angles.

Me) and **14** ($R^1R^2N = NH_2$, and MeNH), but are 69.6° for **14** ($R^1R^2N = Me_2N$) and 67.1° and 76.3° for **16** ($R = H$ and Me), respectively.

The cause of the (1.7×10^3) -fold lesser reactivity in ring closure of the tethered bisketene **16** ($R = Me$) compared to **14** ($R^1R^2N = Me_2N$) does not appear to be due to electronic effects, as the nitrogen in both cases is calculated to be planarized and coplanar with the cyclobutenedione, and pyramidalized in the bisketenes. However, in the dialkylamino cyclobutenedione **13** ($R^1R^2N = Me_2N$) the calculated bond angle $Me_2N-C=C$ is 139.0° , while for the tethered dialkylamino cyclobutenedione **15** ($R = Me$) the corresponding angle $N-C=C$ is constrained to an angle of 124.2° . This angle strain in the tethered cyclobutenedione is a plausible candidate for the cause of the lower reactivity in ring closure of the corresponding bisketene.

In summary 1,2-bis(amino)-substituted 1,2-bisketenes with both free and tethered substituents have been generated, and their ring closure to the corresponding cyclobutenediones has been observed by spectroscopic methods for the first time. The bisketene **14** ($R^1R^2N = Me_2N$) is the most reactive bisketene in ring closure to the corresponding cyclobutenedione that has been measured, in stark contrast to the stability of the highly crowded stable aminoketenes **1** and **2**,¹ and there is an enormous range in reactivities of more than 10^{13} in measured rate constants for ring closure of 1,2-bisketenes. A semiquantitative correlation of the reactivities is found based on substituent parameters SE, and calculations of barriers for ring closure with DFT methods are largely consistent with the results. Ring strain in the tethered cyclobutenediones **15** appears to inhibit their reformation by ring closure.

Experimental Section

The cyclobutenediones **13a** ($R^1R^2N = Me_2N$),^{9b} **13b** ($R^1R^2N = MeNH$),^{9b} **13c** ($R^1R^2N = NH_2$),^{9d} **13d** ($R^1R^2N = PhNH$),^{9b,d} and **15** ($R = Me$)^{9h} are known compounds prepared by literature procedures.

2,5-Di-*n*-butyl-2,5-diazabicyclo[4.2.0]oct-1(6)-ene-7,8-dione (15, R = *n*-Bu). To a stirred solution of diethyl squarate (196 mg, 1.15 mmol) in dry Et₂O (10 mL) was added a solution of *N,N'*-di-*n*-butylethylenediamine (199 mg, 1.15 mmol) in dry Et₂O (5 mL). The mixture was stirred at room temperature overnight and then concentrated under reduced pressure. To the residue was added THF (75 mL) and the solution was refluxed overnight and concentrated

under reduced pressure. The residue was purified by flash chromatography (silica gel, EtOAc/hexanes 2:1 v/v to EtOAc) to afford **15** ($R = n$ -Bu) (162 mg, 56%) as white crystals, mp 185.5 – $186.5^\circ C$. ¹H NMR (400 MHz, CDCl₃) δ 3.51 (t, 4H, $J = 6.8$ Hz), 3.42 (s, 4H), 1.63–1.71 (m, 4H), 1.30–1.41 (m, 4H), 0.95 (t, 6H, $J = 7.6$ Hz). ¹³C NMR (100 MHz, CDCl₃) δ 180.5, 167.6, 51.0, 45.5, 30.3, 19.9, 13.9. EIMS (m/z) 250 (M^+), 179, 151, 137, 111, 96. HREIMS (m/z) calcd for C₁₄H₂₂N₂O₂ 250.1681, found 250.1685. IR (KBr) 1593 cm⁻¹. UV/vis (isooctane) λ_{max} (ϵ) 278 nm (3.65×10^4), 300 nm (4.00×10^4).

Kinetic Measurements. Kinetic measurements by UV spectroscopy of the reformation of cyclobutenones **13** and **15** from bisketenes **14** ($R^1R^2N = MeNH$, NH₂, PhNH) and **16** ($R = Me$ and *n*-Bu), respectively, were measured at the University of Toronto with apparatus described previously.^{10a,b} Cyclobutenedione photolysis with an excimer laser (XeCl, 308 nm) was used to generate the transient bisketenes, except for **13** ($R^1R^2N = MeNH$), for which a Nd:YAG laser (266 nm) was employed, with observation of the reformation of the cyclobutenedione absorption. Substrate concentrations of 5×10^{-6} M (**13**, $R^1R^2N = NH_2$), 5.7×10^{-5} M (**13**, $R^1R^2N = MeNH$), 4.0×10^{-5} M (**13**, $R^1R^2N = PhNH$), $(1.5 \text{ to } 5.8) \times 10^{-6}$ M (**15**, $R = Me$), and 3.5×10^{-6} to 2×10^{-5} M (**15**, $R = n$ -Bu) were used, with either 1 or 5 cm cells. Kinetic measurements by UV spectroscopy on **14** ($R^1R^2N = Me_2N$) were carried out at the University of Georgia, LFP experiments were conducted with ca. 5×10^{-5} M solutions of the substrate in HPLC-grade acetonitrile (5 μ L of 0.02 M stock solution in DMSO was injected into 2 mL of acetonitrile). For excitation the 355 nm frequency tripled output of a Nd:YAG laser was employed. Reformation of absorption of **13** ($R^1R^2N = Me_2N$) was observed at 330 nm.

Kinetic measurements on **16** ($R = n$ -Bu) by IR were carried out in Japan with ketene generation with a Nd:YAG laser (266 nm) and 1.0×10^{-3} M solutions with observations at 2064 and 2116 cm⁻¹.

Acknowledgment. Financial support by the Natural Sciences and Engineering Research Council of Canada and the Petroleum Research Fund, administered by the American Chemical Society, is gratefully acknowledged. Computations were carried out with the High-Performance Computer Cluster at the University of Toronto at Scarborough.

Supporting Information Available: Experimental and computational details. This material is available free of charge via the Internet at <http://pubs.acs.org>.

JO062090H